Sebastian Dietrich[1,*]
Selina Nieß[1]
Stefan Rönsch[2]
Matthias Kraume[3]

Synthesis of Light Hydrocarbons from Biogas and Hydrogen: Investigation of a Fe-Mn-K/MgO Catalyst

Fischer-Tropsch synthesis of the CO_2 in biogas aims at producing light hydrocarbons and increasing its calorific value for feeding into the grid. Fe catalysts with Mn and K as promoters are supposed to yield high amounts of light hydrocarbons. Using a Fe-Mn-K/MgO catalyst, a parameter screening and long-term experiments were carried out. The catalyst shows, within the examined range, the highest selectivity to C_2–C_4 hydrocarbons at 450 °C, 8 bar(a), and a gas hourly space velocity of 350 h^{-1}. Calcination of the catalyst resulted in a significant drop of activity and an almost complete loss of selectivity to hydrocarbons. Admixture of steam to the reactant gas lowers the tendency to carbon deposition but also promotes the water-gas shift reaction and results in lower yields of hydrocarbons.

This is an open access article under the terms of the Creative Commons Attribution License, which permits use, distribution and reproduction in any medium, provided the original work is properly cited.

Keywords: Biogas, Catalyst, Fischer-Tropsch synthesis, Light hydrocarbons, Power-to-X

Received: January 20, 2020; *accepted:* April 22, 2020

DOI: 10.1002/ceat.202000035

1 Introduction

Upgrading the quality of biogas and feeding it into the existing natural gas grid offers an alternative to direct on-site power generation. Biogas can thus contribute to a demand-oriented power generation and is also available for the mobility, industrial, and heating sectors. As German feed-in requirements for the natural gas grid define certain gas properties [1], conditioning of biomethane is necessary. This pertains mainly to raising the heating value and is usually done by adding fossil liquefied petroleum gas.

An alternative concept for the production of a high-calorific gas (H-gas, defined in [1]) is shown in Fig. 1 and consists of a Fischer-Tropsch synthesis (FTS) downstream of the anaerobic fermentation of biomass and a sulfur removal stage. Depending on the catalyst properties, it may be necessary to add a process step for the conversion of the CO_2 from the biogas to CO. The concept also requires a hydrogen source (e.g., from electrolysis; power-to-gas) and a product separation stage to remove or possibly recycle any remaining components from the raw H-gas.

The design of the different process steps and the complexity of the overall process scheme, however, depends on the performance of the Fischer-Tropsch catalyst applied. Hence, the catalyst has a significant influence on the economics of the process and the feasibility of the concept.

Therefore, the present study aims to investigate a Fe-Mn-K/MgO catalyst regarding its performance in the context of the proposed concept. The catalyst was tested at different temperatures, pressures, and gas hourly space velocities (GHSV), in order to determine the optimal process conditions for high conversion rates and selectivity to light alkenes and alkanes

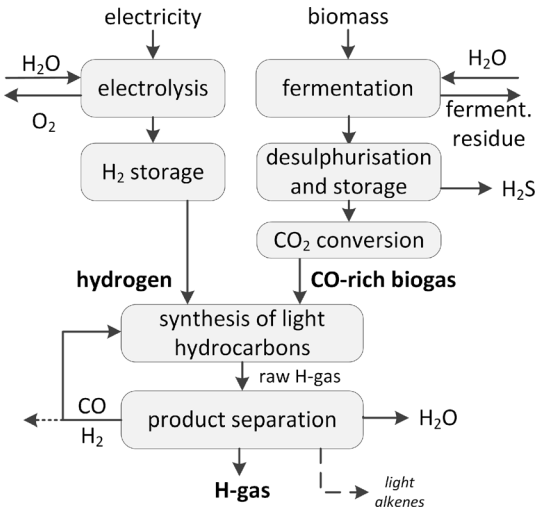

Figure 1. Simplified process scheme for the synthesis of light hydrocarbons to produce a high-calorific gas (H-gas).

[1]Sebastian Dietrich, Selina Nieß
sebastian.dietrich@dbfz.de
DBFZ Deutsches Biomasseforschungszentrum gemeinnützige GmbH (German Centre for Biomass Research), Biorefineries, Torgauer Strasse 116, 04347 Leipzig, Germany.

[2]Prof. Stefan Rönsch
Jena University of Applied Sciences, Department of Industrial Engineering, Carl-Zeiß-Promenade 2, 07745 Jena, Germany.

[3]Prof. Matthias Kraume
TU Berlin, Fachgebiet Verfahrenstechnik, Straße des 17. Juni 135, 10623 Berlin, Germany.

(C_2–C_4). Furthermore long-term experimental runs were conducted to compare the performance of the catalyst at different specific surface areas and to compare the catalyst performance with and without steam admixture to the reactant gas.

1.1 Fischer-Tropsch Synthesis

The FTS was developed in 1926 by Franz Fischer and Hans Tropsch to synthesize liquid hydrocarbons by utilizing a synthesis gas generated from coal [2]. Other suitable raw materials are natural gas as well as biogas, wood, agricultural waste, or household waste [3–5]. The main products of the synthesis are, depending on the process temperature, waxes in a low-temperature approach (200–240 °C) and gasoline and diesel in a high-temperature approach (300–350 °C) [6, 7]. According to [8], light hydrocarbons (mainly C_2–C_4) can be produced at GHSV above 300 h^{-1}, temperatures below 500 °C for supported catalysts, and an H_2/CO ratio between 1 and 3.

The reactions (1) and (2) describe the reaction pathways by which hydrocarbons are produced in the FTS.

Alkanes:

$$n\mathrm{CO} + (2n+1)\mathrm{H_2} \rightarrow \mathrm{C_nH_{2n+2}} + n\mathrm{H_2O} \quad (1)$$

Alkenes:

$$n\mathrm{CO} + 2n\mathrm{H_2} \rightarrow \mathrm{C_nH_{2n}} + n\mathrm{H_2O} \quad (2)$$

In recent years, the FTS of light alkenes/olefins, in particular, has been an intensively discussed topic, as they are particularly interesting as basic chemicals for the chemical industry [9, 10].

In addition to the FTS, secondary reactions take place in the synthesis reactor [11]. These are, on the one hand, methanization, which is also described by Eq. (1) but, by general definition, is not part of the FTS. Furthermore, under most process conditions, the water-gas shift (WGS) reaction takes place to a certain extent and converts CO in the presence of water into CO_2 and H_2. This secondary reaction is particularly undesirable when considering the process scheme shown in Fig. 1, since CO_2 was converted into CO prior to the synthesis in order to enable high selectivity to light hydrocarbons. Another reaction widely accompanying the FTS is the dissociation of CO to carbon atoms, which increasingly occurs with high CO partial pressure [12]. The deposition of carbon blocks active sites, leading to deactivation of the catalyst [13].

1.2 Catalysts for FTS

The industrially most relevant catalysts for FTS are based on the active components Fe and Co [14], while other metals like Ru, Rh, and Ni also actively catalyze the FTS [15]. Co-based catalysts are applied to form long carbon chains [16]; Fe-based catalysts yield shorter chain lengths, favoring alkene production [17] and a decreased methane selectivity at higher temperatures [18]. A drawback of Fe catalysts in FTS is, however, the low stability of the catalyst [18]. Deactivation can occur due to different processes like fouling, sintering, poisoning, or phase changes [19]. The surface of Fe catalysts prepared for FTS consists mainly of different iron carbides, iron oxides, and metallic iron [20]. The former two, carbides and oxides, act as active sites for the FTS and WGS reaction, respectively [21]. The precursors of Fischer-Tropsch Fe catalysts are usually made of iron oxides, mainly of hematite (Fe_2O_3), which is formed during the calcination step of the catalyst preparation [22]. Therefore, these catalysts need to undergo an activation process to form carbide species [23].

The addition of promoting metals like Mn or K can also influence the stability [19] and decrease the required time for the conversion of precursors to active catalysts [23]. K is one of the most widely studied promoters for Fe catalysts [21]. Being an electron donor, K provides an electron flow to the catalytically active metal [24], which improves the subsequent electron donation from Fe to CO [18]. The adsorption of H_2, favored over an electron-deficient metal, is however inhibited by the presence of K on the surface [25, 26]. These adsorption phenomena lead to chain growth and higher-alkene selectivity with K as promoter [27]. Manganese was reported to lead to a high selectivity to lower alkenes (C_2–C_4) when used in combination with K [28]. Mn acts similar to K promoters, promoting the dissociative adsorption of CO while suppressing the chemisorption of H_2 [29].

2 Experimental Methodology

This paper aims to investigate the suitability of the used catalyst for the synthesis of light hydrocarbons. Ideally, these can be produced directly from a mixture of biogas and added hydrogen. However, since no measurable amounts of light hydrocarbons could be generated in preliminary tests, the catalyst was tested with synthesis gas consisting of CO and H_2. In a practical application, this would require an additional, relatively costly, upstream process step to convert CO_2 to CO (see Fig. 1).

2.1 Experimental Setup

All experiments were carried out using the continuous-flow synthesis test rig shown in Fig. 2. In the gas mixing segment, CO and H_2 were mixed and fed into the heated reactant gas line. Steam was added to the dry reactant gas by dispensing liquid water with a high-performance liquid chromatography (HPLC) pump and evaporating it in a pipe heater. The tube reactor itself is heated by a vertical split-tube oven. The synthesis product gas then flows through a heated gas line (200 °C) to the gas cooler (4 °C) to separate any condensable components. The system has a maximum operating pressure of 9 bar(a) and is regulated by a pressure control valve. Gas for analysis flows through a filter to remove any remaining liquid components.

In all presented experiments, the product gas was analyzed using a gas chromatography-thermal conductivity detector (GC-WLD; Micro GC Fusion®, Inficon Holding AG) calibrated to detect H_2, N_2, CO, CO_2, CH_4, and alkenes and alkanes from C_2 to C_4.

A cross-section of the tube reactor itself is shown in Fig. 3. The reactor tube (22×2 mm, 400 mm length, 1.4571 stainless

 © 2020 The Authors. Published by WILEY-VCH Verlag GmbH & Co. KGaA.

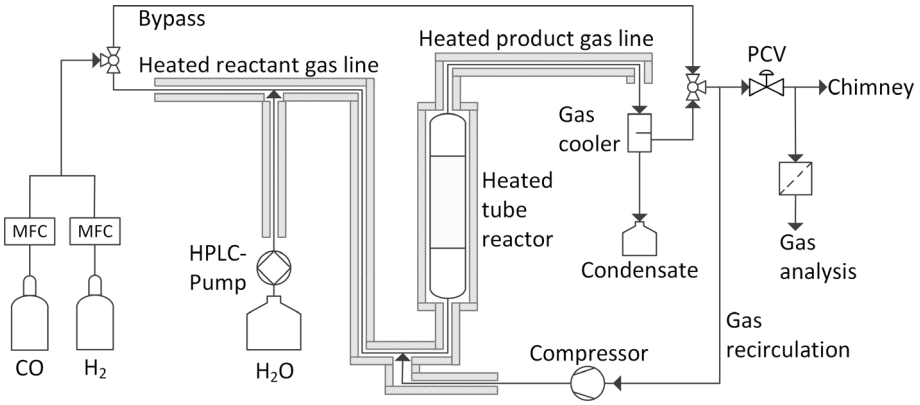

Figure 2. Test rig consisting of a gas mixing segment, steam admixture, a heated tube reactor with heated gas lines, condensate separation, a pressure control valve (PCV), and gas analysis. The entire reactor can be bypassed and a circulation of the product gas is possible.

steel) is connected to the test rig by compression fittings, and in the reactor, there is a tube (6×1 mm) containing ten thermocouples. The catalyst bed is diluted in a ratio of 1:4 with inert material (SiC, carborundum 0.105 mm; VWR Chemicals) and positioned around this inner tube to monitor the temperature gradient within the packed bed. Part of the reactor within the actively heated section of the split-tube oven is filled with pure inert material, in order to further heat up the gas before reaching the catalyst bed. To hold both beds in position, the inlet and outlet of the reactor are packed with silica wool. The catalyst bed (6) as shown in Fig. 3 has a length of approx. 300 mm, containing about 18 g pure catalyst (0.1–0.5 mm). The inert material bed (5) has a length of 70–80 mm.

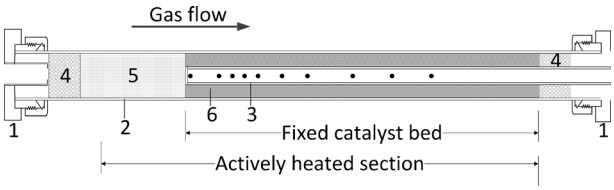

Figure 3. Cross-section of the reactor consisting of compression fittings (1) fixing the reactor tube (2) and an inner tube (3) with ten thermocouples (positions marked by ●). The reactor is filled with silica wool (4), silicon carbide as inert material (5), and the catalyst (6).

2.2 Catalyst

All presented experimental data was gathered using a Fe-Mn-K/MgO catalyst produced by an industrial catalyst manufacturer based on [28, 29] and the results presented in [8]. A Fe catalyst was chosen because of its tendency to yield shorter hydrocarbon chains than Co catalysts.

MgO was impregnated with the metal salt precursors by incipient wetness impregnation in a single step. While K_2CO_3 was previously solved in H_2O, $MnCO_3$ and FeO(OH) were admixed to the support in their solid state and water was added. Mixing was performed in a granulator. The resulting precursors were dried for 6 h at 110 °C.

After preparation, the catalyst had an elemental composition of 11.5 wt % Fe, 10.2 wt % Mn, and 1.1 wt % K, and a Brunauer-Emmett-Teller (BET) surface area of 107 m^2g^{-1}. For one experimental run, this catalyst was calcined for 4 h at 600 °C in air, resulting in a specific surface area of 64 m^2g^{-1}. The BET surface area was determined by N_2 physisorption at −196 °C. Before BET analysis, a sample of approx. 0.2 g was degassed at 90 °C (10 K min^{-1}) for 30 min, then heated to 250 °C with a heating rate of 10 K min^{-1} and held for 12 h.

2.3 Experimental Approach

Each test series began with the activation of the catalyst and a subsequent start-up phase, in which the functional groups are formed on the catalyst. Thereafter, stable operation is possible and the planned process parameters or long-term tests can be examined.

2.3.1 Activation Procedure

The GC-WLD is calibrated with test gases at the beginning of each experimental run. The reactor is purged with 1 L min^{-1} (STP) N_2 to completely flush the system from air and a pressure of 8 bar(a) is built up under this nitrogen flow. The activation procedure itself is then carried out with a reduction agent composed of 50 vol % H_2 and 50 vol % N_2 at a flow rate of 0.2 L min^{-1} (STP). With a ramp of 5 K min^{-1}, the activation temperature of 400 °C is reached and the system is then kept in this state overnight (16–18 h time-on-stream (TOS)).

2.3.2 Start-up Phase

During reduction, the iron oxides are sequentially reduced to magnetite (Fe_3O_4), metastable FeO, and eventually to metallic iron (Sect. 1.2). Contacted with CO or synthesis gas, the metallic iron can be converted into iron carbides associated with a high selectivity to light hydrocarbons. As preliminary tests also showed that this selectivity increased in the first hours of TOS before reaching a stable level, a start-up phase was carried out after activation. During this phase, the pressure was kept at 8 bar(a), the temperature was raised to 450 °C (5 K min^{-1}), and the reactant gas flow rate was set to the maximum flow rate planned for the experiment. The composition and flow rate of the reactant gas are described in Sect. 2.3.3. These conditions were kept constant for all runs over an entire weekend (> 60 h TOS).

 © 2020 The Authors. Published by WILEY-VCH Verlag GmbH & Co. KGaA.

2.3.3 Experimental Designs

All experiments were carried out using a synthesis gas consisting of CO and H_2 in the ratio of 1:1. In order to prevent carbon deposition, 20 vol % steam was admixed in most experimental runs. Therefore, the feed gas composition was 40 vol % CO, 40 vol % H_2, and 20 vol % H_2O when steam was added and 50 vol % CO and 50 vol % H_2 when steam was not added.

2.3.3.1 Parameter Screening

In test run 1 (Tab. 1), a parameter screening was conducted to determine the optimal process conditions for the used Fe-Mn-K/MgO catalyst. This was done by a two-level factorial design with the factors: temperature, pressure, and gas flow rate. During the run, the temperature was set at 350 and 450 °C, the pressure at 1 and 8 bar(a), and the GHSV at 350 and 1150 h^{-1}. In addition, a central point at 400 °C, 4.5 bar(a), and a GHSV of 750 h^{-1} was examined. As all parameter combinations were investigated twice, and the central point, four times, the experiment contained 20 test points in total. The maximum pressure was set to 8 bar(a) since the test rig is not certified for higher pressures. The results are shown and discussed in Sect. 3.1.

2.3.3.2 Influence of Calcination and Water Admixture

Further investigations consisted of long-term experiments, in which the influence of calcination of the used catalyst (test runs 2 and 3) and the influence of the water admixture (test runs 2 and 4) were examined. For this, the original catalyst was calcined as described in Sect. 2.2. In order to investigate the effects of steam addition on the conversion rates and selectivities of the catalyst as well as on the tendency to carbon deposition on the catalyst, a test run with 20 vol % water addition was compared with a long-term test without water addition. Results of these comparisons are shown and discussed in Sects. 3.2 and 3.3.

3 Experimental Results and Discussion

The experimental results are discussed with regard to the influence of the process parameters, calcination of the catalyst, and steam admixture on the synthesis.

3.1 Parameter Screening

The conversion rate of CO ranged, amongst all examined combinations of parameters, from 2.5 % to 76 %. Fig. 4 shows the CO conversion and the respective yields of hydrocarbons and CO_2. The dotted lines represent the predominantly linear progression of the conversion and yields. For CO conversion, there is a strong influence of the pressure and temperature, while the GHSV has a smaller effect (Fig. 4a). Only at maximum pressure and temperature, a more significant difference of about 10 % in conversion rate was determined when comparing the GHSV of 350 and 1150 h^{-1}. By raising the pressure from 1 to 8 bar(a), the CO conversion also rises by 35–36.5 %, except at the maximum temperature and GHSV when the conversion rate only increases by 26.5 %.

Fig. 4b–d shows the yields of C_2–C_4 hydrocarbons, CO_2, and CH_4. While almost no yield (< 2 %) of hydrocarbons could be observed at a pressure of 1 bar(a), maximum yields at 8 bar(a), 450 °C and 350 h^{-1} reached 11.7 % for C_2–C_4 hydrocarbons and 9.3 % for methane. The respective selectivities are 15.3 % for light alkenes and alkanes and 12.1 % for methane. The yields of C_2–C_4 hydrocarbons and CO_2 are, at high pressure, clearly influenced by the temperature and the GHSV. Generally, and within the ranges of the examined parameters, higher temperatures enhance the yield of both methane and light hydrocarbons. The results also show that lower GHSV – and therefore longer residence times – give ample time for the hydrogenation of CO to CH_4 and C_2–C_4 alkenes and alkanes.

All experiments show, at low pressure, almost no selectivity to light hydrocarbons. In contrast to that, even at low pressures, the CO_2 yield reaches 38 % at 450 °C with a selectivity to CO_2 of 96–97 %. CO_2 is formed by the WGS reaction. This reaction is enhanced by the admixed steam, shifting the reaction equilibrium towards the generation of CO_2 and additional H_2. Since the WGS reaction has a strong dependency on the reaction temperature, this effect can already be seen at ambient pressure when the reactor temperature is at 450 °C. Throughout all experimental points, the selectivity to CO_2 was above 72 % (at 8 bar(a), 450 °C, and a GHSV of 350 h^{-1}). The influence of the admixture of steam is further examined and discussed in Sect. 3.3.

With the aim of generating low selectivity to CO_2 and high selectivity to C_2–C_4 alkenes and alkanes, especially the high yields of CO_2 are not satisfactory. For comparison, in [29] different catalysts were observed at 350 °C, 20 bar(a), 1000 h^{-1}, and a CO/H_2 ratio of 2:1. For a catalyst of very similar composition but supported on a silicalite-2 zeolite, a selectivity of 61.4 % to C_2–C_4 hydrocarbons, 38.6 % to CH_4, and no selectiv-

Table 1. Overview of the process parameters for the test runs.

Test run	Description	Pressure [bar(a)]	Temperature [°C]	GHSV [h^{-1}]	Steam admixture	Catalyst state
1	Parameter screening	1, 4.5, 8	350, 400, 450	350, 750, 1150	Yes	Dried
2	Long-term	8	450	350	Yes	Dried
3	Long-term	8	450	350	Yes	Dried and calcined
4	Long-term	8	450	350	No	Dried

 © 2020 The Authors. Published by WILEY-VCH Verlag GmbH & Co. KGaA.

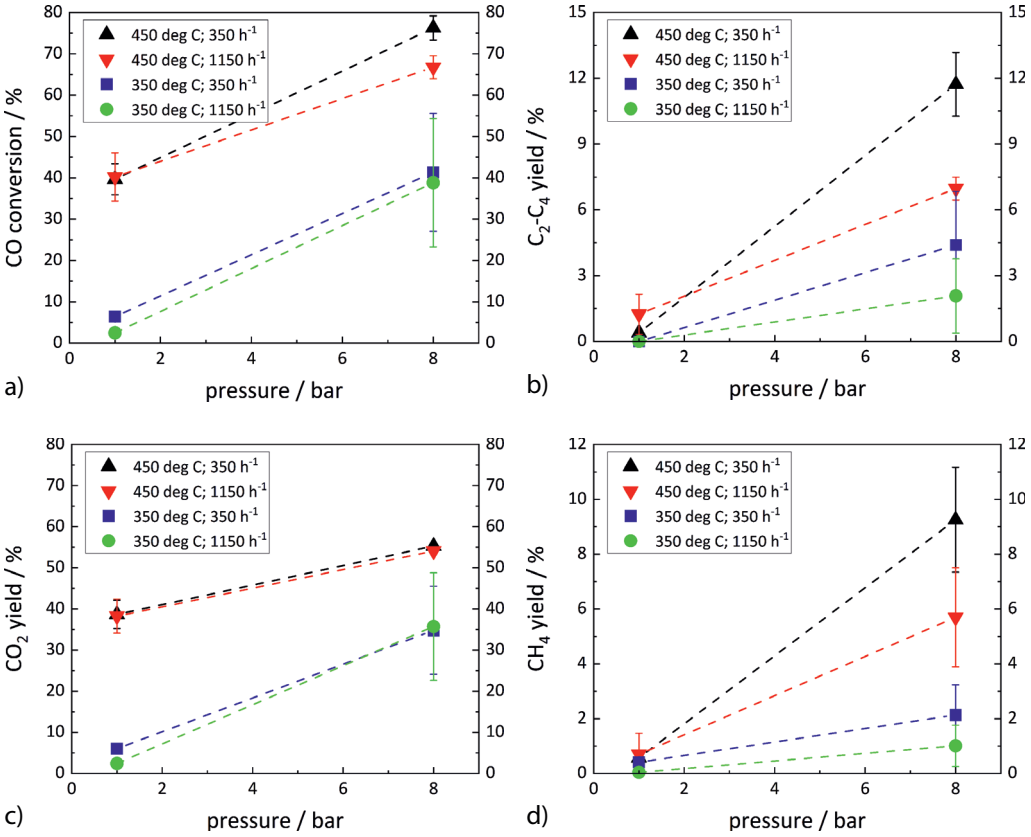

Figure 4. CO conversion (a), C_2–C_4 alkane and alkene yield (b), CO_2 yield (c), and CH_4 yield (d) in the range of $p = 1$–8 bar(a), 350–450 °C, and GHSV = 350–450 h^{-1} in a diluted catalyst bed (1:4). The error bars indicate the variation of the measured values around the mean value.

ity to CO_2 at all were reported. In an earlier study [8], a CO_2 selectivity of 59–74 % was achieved at 440 °C and 160 h^{-1} for a Fe-Mn/MgO catalyst at CO conversion rates of 18–44 %. The selectivity, without steam injection, to light alkenes and alkanes was at 18.5 % higher than in the results presented (15.3 %, with steam injection). The results from Sect. 3.3 serve to improve comparability.

3.2 Influence of Calcination

Long-term experiments were carried out to examine the characteristics of the Fe-Mn-K/MgO catalyst before and after calcination in air (as described in Sect. 2.2). Fig. 5a shows that, after calcination (specific surface area of 64 m^2g^{-1}), no selectivity to hydrocarbons could be measured. Therefore, the values for CO conversion and CO_2 yield overlap almost completely. Due to the erratic water addition (discussed in Sect. 3.3), the conversion rates fluctuated strongly, ranging between 35 % and 40 % over the entire test period of about 90 h TOS.

The long-term test before calcination (specific catalyst surface area of 107 m^2g^{-1}) shows significantly higher CO conversion rates of 70–75 % and C_2–C_4 yields of around 10 %. As shown in Fig. 5b, it takes about 10 h from the start of the test until stable conditions are achieved for the synthesis. Furthermore, it seems as if there is a slight reduction of the CO conversion rate over the course of the long-term experiment.

Based on these results, it can be concluded that calcination has a fairly strong impact on the selectivity to hydrocarbons in particular. However, the higher catalyst activity also seems to lead to a higher tendency towards deactivation.

3.3 Influence of Water Admixture

A comparison of the synthesis reaction with 20 vol % and without steam injection is shown in Fig. 6. The effect of the shift in equilibrium of the WGS reaction to the products, which has already been discussed in Sect. 3.1, is clearly visible. Although the CO conversion rate without water addition (Fig. 6a) is at 50–60 % lower than with water addition (Fig. 6b), the yield of C_2–C_4 alkenes and alkanes increases significantly up to 20 % if no additional steam is fed into the reactor. Also, without steam injection, the selectivity to CO_2 decreases from about 80 % to about 60 % and the selectivity to light hydrocarbons increases from about 15 % to 20 %.

A significantly lower fluctuation of the measured values is clearly noticeable when no steam is added to the reactant gas. Although the HPLC pump doses smallest amounts of water

 © 2020 The Authors. Published by WILEY-VCH Verlag GmbH & Co. KGaA.

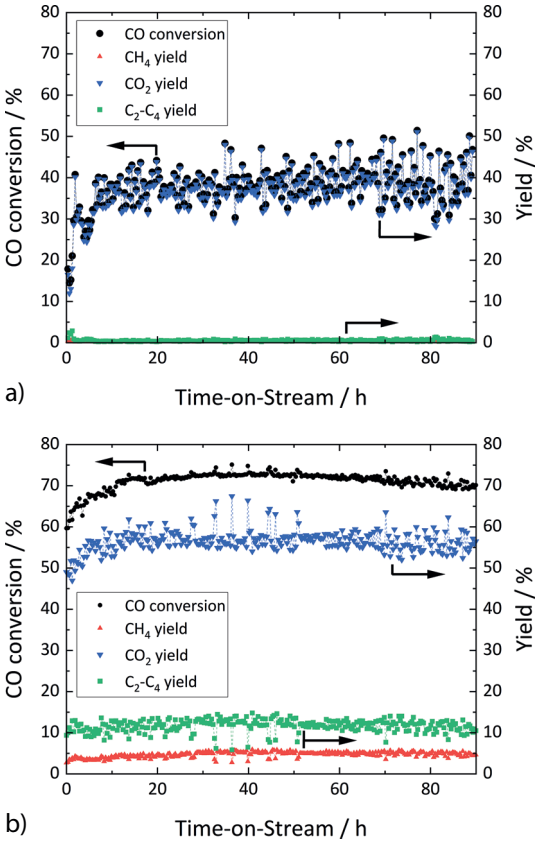

Figure 5. Comparison of the calcined (a) (test run 3) and not calcined catalyst (b) (test run 2) over 90 h TOS at 450 °C and 8 bar(a), for a diluted catalyst bed (1:4) at 350 h^{-1}.

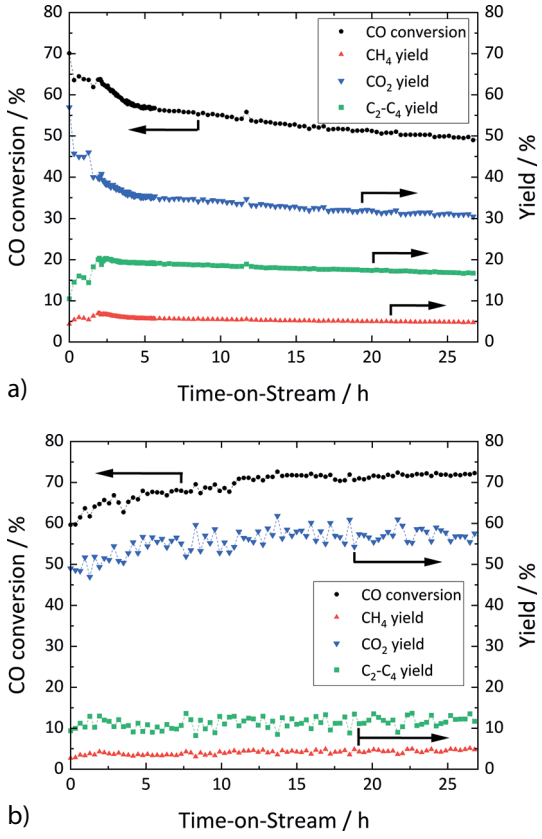

Figure 6. Comparison of steam admixture of 0 vol % (a) (test run 4) and 20 vol % (b) (test run 2) over 27 h TOS at 450 °C and 8 bar(a), for a diluted catalyst bed (1:4) at 350 h^{-1}.

into the system at a frequency of < 1 s, the water then appears to evaporate very unevenly in the heated reactant gas line and is therefore added irregularly to the CO/H_2 mixture.

While the results of the synthesis without water addition are clearly better in terms of producing light hydrocarbons, it must be noted that a decrease in catalyst activity is already visible over the duration of the experiment. The lack of water addition seems to lead to an increased Boudouard reaction causing carbon depositions on the active sites of the catalyst. This became apparent by an increasing pressure difference over time when comparing the pressure at the inlet and outlet of the reactor. It was also noticed when disposing the used catalyst after the experimental runs.

For commercial use, the catalyst would either have to be regenerated in short intervals or an optimum amount of steam admixture has to be found in order to achieve both a high selectivity to alkenes and alkanes and a low tendency for carbon depositions. However, it is more appropriate to screen for a catalyst that is active at lower temperatures, at which the WGS reaction has a minor impact on the synthesis reaction.

4 Conclusion and Outlook

The parameter screening showed that, at low pressures, CO is only converted in small rates and no significant selectivity to hydrocarbons could be observed. The highest CO conversion (76 %) and also the highest selectivity to hydrocarbons (11.7 % for C_2–C_4 hydrocarbons and 9.3 % for CH_4) were achieved at maximum temperature (450 °C), maximum pressure (8 bar(a)), and the lowest GHSV (350 h^{-1}). As the GHSV has a strong influence on the selectivity to hydrocarbons but almost no influence on the selectivity to CO_2, this is a very good variable for optimizing the process.

The non-calcined catalyst has a significantly higher selectivity to C_2–C_4 alkenes and alkanes, as well as a lower selectivity to CO_2. In order to avoid a high WGS activity, steam should not be admixed to the synthesis gas. Experiments without steam admixture reached the overall highest yields of light hydrocarbons (20 %). The drawback is, most likely due to carbon deposition, a visible decrease in activity within the first 27 h TOS.

Higher synthesis temperatures are technically possible and the optimum selectivity to hydrocarbons seems to be above 450 °C. Raising the temperature further is not recommendable due to increased WGS activity. It would be more reasonable to increase the reaction pressure or lower the GHSV to obtain higher selectivities to hydrocarbons, but this is, with regard to the economic feasibility of the overall, decentralized concept in combination with small-scale biogas plants, not advisable. Based on the results obtained, the catalyst used does not appear to be especially suitable for the synthesis of light hydrocarbons

 © 2020 The Authors. Published by WILEY-VCH Verlag GmbH & Co. KGaA.

from biogas. For a better assessment, studies on a comparative catalyst and an economic feasibility study will be carried out.

Acknowledgment

The authors thank the Sächsische Aufbaubank (SAB) for funding the project "Fermenthen", in which the results presented here were produced. Furthermore, we thank the industrial catalyst manufacturer for the supply of the catalyst used.

The authors have declared no conflict of interest.

Abbreviations

FTS	Fischer-Tropsch synthesis
GC-WLD	gas chromatography-thermal conductivity detector
GHSV	gas hourly space velocity
HPLC	high-performance liquid chromatography
STP	standard temperature and pressure
TOS	time-on-stream
WGS	water-gas shift reaction

References

[1] DVGW G 260 (A), *Gasbeschaffenheit*, Deutscher Verein des Gas- und Wasserfaches e.V.: Technische Regeln, Bonn **2013**.

[2] H. Mahmoudi, M. Mahmoudi, O. Doustdar, H. Jahangiri, A. Tsolakis, S. Gu, M. L. Wyszynski, *Biofuels Eng.* **2017**, *2 (1)*, 11–31. DOI: https://doi.org/10.1515/bfuel-2017-0002

[3] S. S. Ail, S. Dasappa, *Renewable Sustainable Energy Rev.* **2016**, *58*, 267–286. DOI: https://doi.org/10.1016/j.rser.2015.12.143

[4] A. S. Snehesh, H. S. Mukunda, S. Mahapatra, S. Dasappa, *Energy* **2017**, *130*, 182–191. DOI: https://doi.org/10.1016/j.energy.2017.04.101

[5] R. G. dos Santos, A. C. Alencar, *Int. J. Hydrogen Energy* **2019**, in press. DOI: https://doi.org/10.1016/j.ijhydene.2019.07.133

[6] B. Jager, R. Espinoza, *Catal. Today* **1995**, *23 (1)*, 17–28. DOI: https://doi.org/10.1016/0920-5861(94)00136-p

[7] A. de Klerk, E. Furimsky, *Catalysis in the Refining of Fischer-Tropsch Syncrude*, 4th ed., RSC Catalysis Series, Royal Society of Chemistry, Cambridge **2010**. DOI: https://doi.org/10.1039/9781849732017-00270

[8] J. Schneider, M. Struve, U. Trommler, M. Schlüter, L. Seidel, S. Dietrich, S. Rönsch, *Fuel Process. Technol.* **2018**, *170*, 64–78. DOI: https://doi.org/10.1016/j.fuproc.2017.10.018

[9] H. M. Torres Galvis, K. P. de Jong, *ACS Catal.* **2013**, *3 (9)*, 2130–2149. DOI: https://doi.org/10.1021/cs4003436

[10] Z. Hu, Z. Ou, L. Yang, F. Gao, B. Xu, Q. Wu, Y. Fan, Y. Zhang, Y. Jiang, R. Huang, X. Wang, Z. Hu, *Chem. Sci.* **2019**, *10*, 6083–6090. DOI: https://doi.org/10.1039/c9sc01210a

[11] C. K. Rofer-DePoorter, *Chem. Rev.* **1981**, *81 (5)*, 447–474. DOI: https://doi.org/10.1021/cr00045a002

[12] M. Ding, Y. Yang, J. Xu, Z. Tao, H. Wang, H. Wang, H. Xiang, Y. Li, *Appl. Catal., A* **2008**, *345 (2)*, 176–184. DOI: https://doi.org/10.1016/j.apcata.2008.04.036

[13] S. Soled, E. Iglesia, R. A. Fiato, *Catal. Lett.* **1990**, *7 (1–4)*, 271–280. DOI: https://doi.org/10.1007/bf00764508

[14] B. Todic, L. Nowicki, N. Nikacevic, D. B. Bukur, *Catal. Today* **2016**, *261*, 28–39. DOI: https://doi.org/10.1016/j.cattod.2015.09.005

[15] P. M. Maitlis, A. de Klerk, *Greener Fischer-Tropsch Processes: For Fuels and Feedstocks*, Wiley-VCH Verlag, Weinheim **2013**. DOI: https://doi.org/10.1002/9783527656837

[16] G. J. Kelly, in *Hydrogenation* (Ed: S. D. Jackson), De Gruyter, Boston **2018**, 155–172. DOI: https://doi.org/10.1515/9783110545210-006

[17] F. Jiao, J. Li, X. Pan, J. Xiao, H. Li, H. Ma, M. Wei, Y. Pan, Z. Zhou, M. Li, S. Miao, J. Li, Y. Zhu, D. Xiao, T. He, J. Yang, F. Qi, Q. Fu, X. Bao, *Science* **2016**, *351 (6277)*, 1065–1068. DOI: https://doi.org/10.1126/science.aaf1835

[18] Y. Cheng, J. Lin, K. Xu, H. Wang, X. Yao, Y. Pei, S. Yan, M. Qiao, B. Zong, *ACS Catal.* **2016**, *6*, 389–399. DOI: https://doi.org/10.1021/acscatal.5b02024

[19] J. van de Loosdrecht, I. M. Ciobîcă, P. Gibson, N. S. Govender, D. J. Moodley, A. M. Saib, C. J. Weststrate, J. W. Niemantsverdriet, *ACS Catal.* **2016**, *6*, 3840–3855. DOI: https://doi.org/10.1021/acscatal.6b00595

[20] T. Riedel, H. Schulz, G. Schaub, K.-W. Jun, J.-S. Hwang, K.-W. Lee, *Top. Catal.* **2003**, *26*, 41–54. DOI: https://doi.org/10.1023/b:toca.0000012986.46680.28

[21] M. Amoyal, R. Vidruk-Nehemya, M. V. Landau, M. Herskowitz, *J. Catal.* **2017**, *348*, 29–39. DOI: https://doi.org/10.1016/j.jcat.2017.01.020

[22] A. V. Puga, *Catal. Sci. Technol.* **2018**, *8 (22)*, 5681–5707. DOI: https://doi.org/10.1039/c8cy01216d

[23] S. Li, R. J. O'Brian, G. D. Meitzner, H. Hamdeh, B. H. Davis, E. Iglesia, *Appl. Catal., A* **2001**, *219*, 215–222. DOI: https://doi.org/10.1016/s0926-860x(01)00694-9

[24] J. Hagen, *Industrial Catalysis: A Practical Approach*, Wiley-VCH Verlag, Weinheim **2006**. DOI: https://doi.org/10.1002/cjce.5450840516

[25] S. Li, A. Li, S. Krishnamoorthy, E. Iglesia, *Catal. Lett.* **2001**, *77 (4)*, 197–205. DOI: https://doi.org/10.1023/a:1013284217689

[26] W. Ma, E. L. Kugler, D. B. Dadyburjor, *Energy Fuels* **2007**, *21 (4)*, 1832–1842. DOI: https://doi.org/10.1021/ef060654e

[27] F. Jiang, M. Zhang, B. Liu, Y. Xu, X. Liu, *Catal. Sci. Technol.* **2017**, *7 (5)*, 1245–1265. DOI: https://doi.org/10.1039/c7cy00048k

[28] L. Xu, Q. Wang, Y. Xu, J. Huang, *Catal. Lett.* **1995**, *31 (2/3)*, 253–266. DOI: https://doi.org/10.1007/bf00808838

[29] L. Xu, Q. Wang, Y. Xu, J. Huang, *Catal. Lett.* **1994**, *24 (1/2)*, 177–185. DOI: https://doi.org/10.1007/bf00807388

 © 2020 The Authors. Published by WILEY-VCH Verlag GmbH & Co. KGaA.